A Computationally-Efficient Two-Step Implementation of the GLRT Detector

Nicholas Pulsone and Michael Zatman, MIT Lincoln Laboratory, 244 Wood St. Lexington, MA 02420

Abstract

In this paper, a new two-step implementation of the GLRT is proposed. A disadvantage of the GLRT detector is that it is more computationally complex than the simple AMF detector. Our two-step implementation of the GLRT significantly reduces the computational load with a negligible loss in detection performance.

1. Introduction

The Adaptive Matched Filter (AMF) [1], Generalized Likelihood Ratio Test (GLRT) [2], and Adaptive Coherency Estimator (ACE) [3,4] are well known CFAR detection schemes. The GLRT is known to be the benchmark detector for a multivariate complex-Gaussian noise environment. More recently, the Adaptive Sidelobe Blanker (ASB), a two stage test was proposed [5,6], consisting of an AMF test followed by an ACE test on anything that passes the AMF test. Here we propose a similar two stage implementation of the GLRT, i.e. an AMF test followed by a GLRT test.

In this paper we show that a two stage implementation of the GLRT achieves significant computational savings with a minimal loss in detector performance. The paper is organized as follows. In section 2 we describe the various detectors and their computational requirements, followed by an analysis of the two-step GLRT's performance in section 3. In section 4 we present simulation results that confirm the validity of our analysis, and draw conclusions in section 5.

2. Adaptive Detection

In this paper the radar signal processing model is used, where the NxN sample noise covariance matrix, $\hat{\boldsymbol{R}}$, is estimated from K snapshots of secondary data, i.e. data other than $\boldsymbol{x}$, the data vector under test. The usual multivariate complex-Gaussian model for the noise is assumed.

This work was sponsored by the United States Navy under Air Force Contract F19628-95-C-0002. Opinions, interpretations, conclusions and recommendations are those of the author, and are not necessarily endorsed by the United States Air Force or the United States Navy.

Three one-step detectors which have been proposed are the AMF

$$t_{AMF} = \frac{\left|\boldsymbol{v}^H \hat{\boldsymbol{S}}^{-1}\boldsymbol{x}\right|^2}{\boldsymbol{v}^H \hat{\boldsymbol{S}}^{-1}\boldsymbol{v}} \gtrless \eta_{AMF}, \tag{1}$$

the GLRT,

$$t_{GLRT} = \frac{t_{AMF}}{1+\boldsymbol{x}^H \hat{\boldsymbol{S}}^{-1}\boldsymbol{x}} \gtrless \eta_{GLRT}, \tag{2}$$

and the ACE

$$t_{ACE} = \frac{t_{AMF}}{\boldsymbol{x}^H \hat{\boldsymbol{S}}^{-1}\boldsymbol{x}} \gtrless \eta_{ACE}, \tag{3}$$

where $\hat{\boldsymbol{S}} = K\hat{\boldsymbol{R}}$.

The relationship between the AMF and the other detectors is clear from the equations above. The GLRT is considered to be the benchmark detector for the multivariate complex-Gaussian signal model. While the ACE detector does not performs as well at high SINRs [3], for some non-Gaussian noise models the ACE detector is a large dimension approximation of the AMF [4].

Typically the AMF weight vector, $\boldsymbol{w} = \hat{\boldsymbol{R}}^{-1}\boldsymbol{v}$, is computed by performing a QR decomposition on the data ($8N^2(K\text{-}N/3)$ flops) and two back-substitutions ($8N^2$ flops). Applying the weights to each snapshot under test (a vector inner product) takes $8N$ flops. By comparison the GLRT and ACE require an additional two back-substitutions and an additional inner product for each snapshot under test.

The two step ASB first performs an AMF test on the data, followed by an ACE test on those snapshots which pass the AMF. Thus the additional back-substitutions and vector inner product are only required for a much smaller number of snapshots. Furthermore, the ASB can provide detection performance better than either the AMF or ACE detectors alone by careful choice of the thresholds [5]. The optimal choice of thresholds provides GLRT like performance, but depends on the unknown target signal-to-interference noise ratio (SINR).

In a similar fashion, the two-step GLRT detector proposed here follows an AMF test on all the data with a GLRT test on those snapshots which pass the AMF test. This vastly reduces the number of back-substitutions and complex multiplies required. Furthermore, we show in the

next sections that the two step detector has detection performance commensurate to the one-step GLRT for practically all useful scenarios, and in contrast to the ASB, the optimum choice of thresholds is not a function of the target SINR.

3. Theoretical Performance Evaluation

In this section we derive expressions for the probability of detection and the probability of false alarm for the two-step GLRT detector. To simplify the analysis we use the following form of the GLRT detector

$$\tilde{t}_{GLRT} = \frac{1 + \boldsymbol{x}^H \hat{\boldsymbol{S}}^{-1} \boldsymbol{x}}{1 + \boldsymbol{x}^H \hat{\boldsymbol{S}}^{-1} \boldsymbol{x} - \dfrac{\left| \boldsymbol{v}^H \hat{\boldsymbol{S}}^{-1} \boldsymbol{x} \right|^2}{\boldsymbol{v}^H \hat{\boldsymbol{S}}^{-1} \boldsymbol{v}}} \gtrless \tilde{\eta}_{GLRT} \quad ,$$

$$\text{i.e. } \tilde{t}_{GLRT} = \frac{1}{1 - t_{GLRT}} \text{ and } \tilde{\eta}_{GLRT} = \frac{1}{1 - \eta_{GLRT}} \quad , \tag{4}$$

which is statistically equivalent to the test given in (2).

Our derivation follows the analysis of the ASB given in [5,6] and uses similar notation. For convenience we relate the distribution of the AMF test statistic t_{AMF} given in [1] and the GLRT test statistic t_{GLRT} given in [2] in terms of two related random quantities, a complex non-central F-distributed random variable and a complex central β-distributed random variable as follows

$$t_{AMF} \triangleq \frac{F_{1,L}(\delta_\beta)}{\beta_{L+1,N-1}} \quad , \tag{5}$$

$$\tilde{t}_{GLRT} \triangleq F_{1,L}(\delta_\beta) + 1 \quad , \tag{6}$$

where the symbol $\triangleq$ denotes equality in distribution and δ_β is related to the SINR $\alpha \equiv |a|^2 \boldsymbol{v}^H \boldsymbol{R}^{-1} \boldsymbol{v}$, $\delta_\beta^2 \equiv \alpha \cdot \beta_{L+1,N-1}$. We assume that $\boldsymbol{v}$ has unit norm, i.e. $\boldsymbol{v}^H \boldsymbol{v} = 1$ and we introduce the integer $L \equiv K - N + 1$. Note that the two random quantities used to describe the distributions of the test statistics are related by $\beta_{L+1,N-1}$ which is often referred to as the loss factor [1,2,5,6]. The probability density function for $\beta_{L+1,N-1}$ is

$$f_B(\beta) = \frac{K!}{L!(N-2)!} \beta^L (1-\beta)^{N-2}, \quad 0 \le \beta \le 1 \quad . \tag{7}$$

3.1 The Probability of Detection

The two-step GLRT detector declares a target signal present in the data vector under test if both the AMF test statistic and the GLRT test statistic exceed their respective thresholds, i.e. $t_{AMF} > \eta_{AMF}$ and $t_{GLRT} > \eta_{GLRT}$. Consequently the probability of detection (P_D) for the two-step GLRT detector is given by,

$$P_D = \Pr(t_{AMF} > \eta_{AMF}, \tilde{t}_{GLRT} > \tilde{\eta}_{GLRT}) \, . \tag{8}$$

By using the random quantities given in (5) and (6) we can express the P_D given in (8) conditioned on the loss factor β,

$$P_D = \int_0^1 \Pr(F_{1,L}(\delta_\beta) > \eta_{AMF} \, \beta, \; F_{1,L}(\delta_\beta) > \tilde{\eta}_{GLRT} - 1 | \beta) \cdot f_B(\beta) \, d\beta \, , \tag{9}$$

or equivalently,

$$P_D = \int_0^1 \Pr(F_{1,L}(\delta_\beta) > \max[\eta_{AMF} \, \beta, \tilde{\eta}_{GLRT} - 1] | \beta) \cdot f_B(\beta) \, d\beta \quad . \tag{10}$$

By defining a the parameter γ as follows

$$\gamma \equiv \begin{cases} 1 & \tilde{\eta}_{GLRT} - 1 \ge \eta_{AMF} \\ \dfrac{\tilde{\eta}_{GLRT} - 1}{\eta_{AMF}} & otherwise \end{cases} \quad , \tag{11}$$

we can express the P_D given in (9) as follows

$$P_D = \int_0^\gamma P_D^{GLRT} | \beta \cdot f_B(\beta) \, d\beta + \int_\gamma^1 P_D^{AMF} | \beta \cdot f_B(\beta) \, d\beta \quad , \tag{12}$$

where $P_D^{GLRT} | \beta$ and $P_D^{AMF} | \beta$ are the conditional probabilities of detection for the GLRT and the AMF tests respectively. From [5,6] these conditional probabilities are expressible as finite sums

$$P_D^{GLRT} | \beta = 1 - \frac{1}{(\tilde{\eta}_{GLRT})^{K-1}} \sum_{m=1}^{L} \binom{L}{m} (\tilde{\eta}_{GLRT} - 1)^m G_m\left(\frac{\delta_\beta^2}{\tilde{\eta}_{GLRT}} \right), \tag{13}$$

$$P_D^{AMF} | \beta = 1 - \frac{1}{(1 + \beta \eta_{AMF})^{K-1}} \sum_{m=1}^{L} \binom{L}{m} (\beta \eta_{AMF})^m \cdot G_m\left(\frac{\delta_\beta^2}{1 + \beta \eta_{AMF}} \right) \, . \tag{14}$$

The function $G_i(x)$ in (13) and (14) is related to the incomplete Gamma function $\Gamma(i,x)$ as follows

$$G_i(x) = \frac{\Gamma(i,x)}{(i-1)!} = e^{-x} \sum_{n=0}^{i-1} \frac{x^n}{n!} \quad . \tag{15}$$

3.2 The Probability of False Alarm

The probability of false alarm (P_{FA}) for the two-step implementation of the GLRT is obtained from (12) by setting the SINR $\alpha = 0$. Hence, the P_{FA} is as follows

$$P_{FA} = \int_0^\gamma P_{FA}^{GLRT} | \beta \cdot f_B(\beta) \, d\beta + \int_\gamma^1 P_{FA}^{AMF} | \beta \cdot f_B(\beta) \, d\beta \quad , \tag{16}$$

where $P_{FA}^{GLRT}|\beta$ and $P_{FA}^{AMF}|\beta$ are the conditional probabilities of false alarm for the GLRT and the AMF tests respectively and are expressible as the following finite sums

$$P_{FA}^{GLRT}|\beta = 1 - \frac{1}{(\tilde{\eta}_{GLRT})^{K-1}} \sum_{m=1}^{L} \binom{L}{m} (\tilde{\eta}_{GLRT} - 1)^m \quad , \tag{17}$$

$$P_{FA}^{AMF}|\beta = 1 - \frac{1}{(1+\beta\eta_{AMF})^{K-1}} \sum_{m=1}^{L} \binom{L}{m} (\beta\eta_{AMF})^m \quad . \tag{18}$$

Note that the P_{FA} due to the GLRT part of the two-stage detection algorithm, i.e. the left hand integral in (16), is independent of β and expressible in terms of the incomplete beta function $I_x(p,q)$ as shown

$$\int_0^{\gamma} P_{FA}^{GLRT}|\beta \cdot f_B(\beta)\, d\beta = \left(\frac{1}{\tilde{\eta}_{GLRT}}\right)^L I_{\gamma}(L+1, N-1) \quad . \tag{19}$$

Furthermore, there are an infinite number of threshold pairs $\tilde{\eta}_{GLRT}$ and η_{AMF} that satisfy (16) for a given P_{FA}.

4. Performance Examples

In this section we show both analytical and simulated probabilities of detection (PD) examples for an N=4 degree of freedom (DOF) adaptive system for various probabilities of false alarm (PFA) and levels of sample support (K - the number of snapshots).

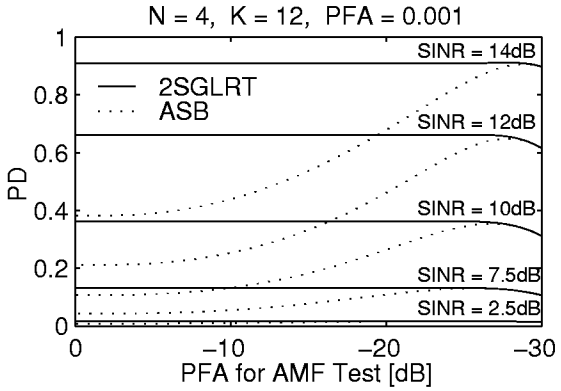

Figure 1: PD of the 2SLGRT and ASB detectors as a function of the AMF test threshold for K=12 secondary data samples, N=4 DOFs and an overall PFA of 10^{-3}.

Figure 1 shows the PD of the two-step GLRT (2SGLRT) and ASB detectors as a function of the AMF test threshold for 12 secondary data samples and an overall two-stage detector PFA of 10^{-3}. (Note that the computational savings realized by the ASB and 2SGLRT relative to ACE and the GLRT grow as the AMF test PFA shrinks.) If the AMF test PFA is 1 (0 dB - left hand side of the plot), then the detector is running as a regular one-step GLRT or ACE. If the AMF PFA is 10^{-3} (-30 dB - right hand side of the plot) then the detector is running as an AMF only detector.

It has previously been reported [5,6] that there is a single choice of AMF and ACE thresholds which maximizes the ASB PD for a particular PFA and target SINR. The fact that the optimal threshold depends on the unknown target SINR is a drawback of the ASB detector. For the most part the 2SGLRT's PD is unaffected by the choice of AMF threshold. Only for high AMF thresholds does the 2SGLRT performance begin to degrade. The ASB's PD quickly degrades from GLRT like performance when the AMF threshold is either higher or lower than the optimum. As expected, both two-step detectors degrade towards pure AMF performance for high levels of the AMF threshold.

Figure 2 shows analytical and *monte-carlo* simulation (MC) plots of detector PD as a function of target SINR for the scenario of Figure 1. For the two-step detectors an AMF PFA of $10^{-2.5}$ was chosen (about optimal for the ASB with a 2.5 dB SINR target). At medium and high target SINRs the 2SGLRT slightly outperforms the ASB detector. The *monte-carlo* simulation results for the 2SGLRT agree with the theoretical results.

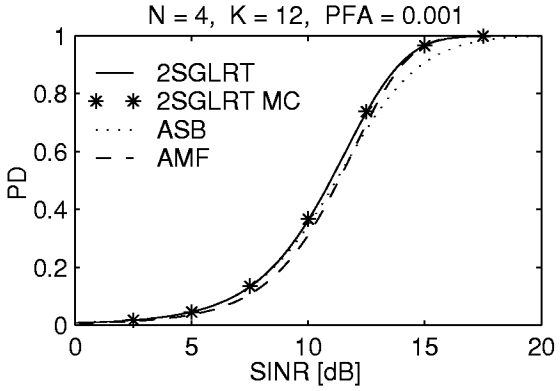

Figure 2: Plots of detector PD as a function of target SINR for the scenario of figure 1. An AMF PFA of $10^{-2.5}$ was used for both two-step detectors. The 2SGLRT slightly outperforms the ASB at medium and high SINRs.

Figure 3 shows the PD of the 2SGLRT and ASB detectors as a function of the AMF test threshold for a total PFA of 10^{-6} and 8 secondary data samples. Similar to the case of Figure 1, for each target SINR there is clearly a single optimum choice of AMF and ACE thresholds for the ASB. The 2SGLRT is much less sensitive to the choice of thresholds, performance only degrading in similar fashion to the ASB for high AMF thresholds.

Figure 4 shows analytical and *monte-carlo* simulation (MC) plots of detector PD as a function of target SINR for

the scenario of Figure 3. AMF PFAs of 10^{-5} for the 2SGLRT and $10^{-5.5}$ for the ASB were used. The $10^{-5.5}$ AMF PFA is optimizes the ASB performance for a 23 dB SINR. Hence in this case the 2SGLRT slightly outperforms the ASB detector at low and medium SINRs. Again, the *monte-carlo* simulation results for the 2SGLRT agree with the theoretical results.

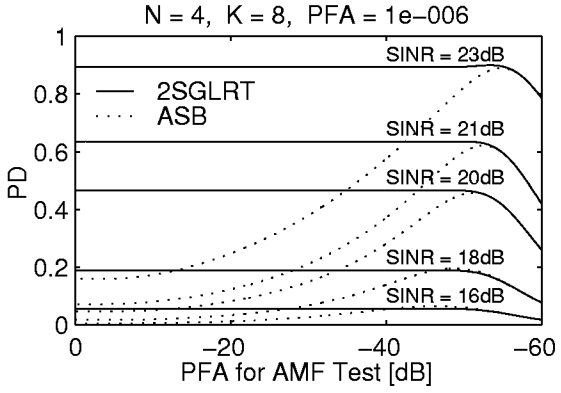

Figure 3: PD of the 2SGLRT and ASB detectors as a function of the AMF test threshold for K=8 secondary data samples, N=4 DOFs and a PFA of 10^{-6}.

In Figure 4 the 2SGLRT is providing the same PD and PFA performance as the regular GLRT, but with only the computation of the AMF plus an average of about $^{1}/_{100000}$ of the additional computation of the regular GLRT (assuming that the number of targets is small and snapshots interrogated large).

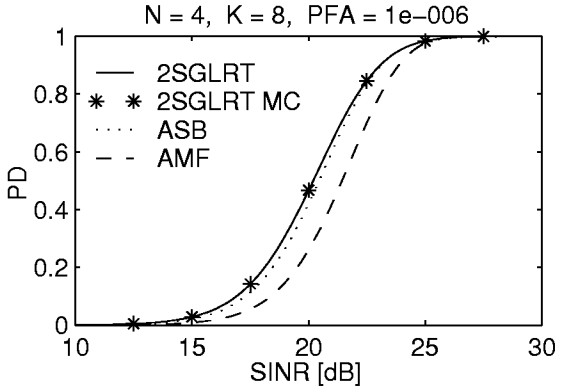

Figure 4: Plots of detector PD as a function of target SINR for the scenario of figure 3. AMF PFAs of 10^{-5} for the 2SGLRT and $10^{-5.5}$ for the ASB were used. At low and medium SINRs the 2SGLRT slightly outperforms the ASB.

5. Summary

In this paper we have presented a new two-step implementation of the GLRT. This implementation provides detection performance commensurate with the regular GLRT while achieving significant computational savings. For the multivariate complex-Gaussian signal model our two-step GLRT has two performance advantages over the other two-step detector examined - the ASB;

1) The choice of threshold pairs that maximizes PD for a given PFA does not depend on the unknown target SINR.

2) For a given PFA the two-step GLRT's performance is constant for a wide range of threshold pairs.

These two advantages explain the slightly improved detection performance of the two-step GLRT over the ASB in the examples reported in this paper.

It has been demonstrated that altering the ASB's thresholds (while keeping the PFA constant), can increase that detector's rejection of 'sidelobe' targets at the expense of the probability of detection of 'mainlobe' targets [6]. This is advantageous in the non-homogenous interference scenarios for which the ASB was designed. Although not proven here, assuming the AMF threshold is not set too high, it can be shown that the two-step GLRT provides sidelobe target rejection commensurate with the regular GLRT, which is less than the maximum sidelobe rejection afforded by the ASB.

References

[1] Robey, F.C., Fuhrmann, D.R., Kelley, E.J. and Nitzberg, R.A., "A CFAR adaptive matched filter detector", *IEEE Trans. AES*, vol. 28 no. 1 pp. 208-216. 1992.

[2] Kelly, E.J. "An adaptive detection algorithm", *IEEE Trans. AES*, vol. 22, no. 1, pp. 115-127, 1986.

[3] Scharf, L.L. and McWhorter, L.T., "Adaptive matched subspace detectors and adaptive coherence", *Proc. 30th Asilomar Conf. on Signals and Systems*, 1996, pp. 1114-1117, also *submitted IEEE Trans. Signal Processing* 1996.

[4] Pulsone, N.B., "Adaptive signal detection non-Gaussian interference", PhD Thesis, *Northeastern University*, May 1997.

[5] Richmond, C.D., "Statistical performance analysis of the adaptive sidelobe blanker detection algorithm", *Proc. 31st Asilomar Conf. on Signals and Systems*, 1997 pp. 872-876, also *submitted IEEE Trans. Sig. Proc.* 1997

[6] Richmond, C. D., "An analysis of an adaptive detection algorithm for non-homogeneous environments", ICASSP 1998, pp. 2005-2008.